

New magnetic resonance imaging based method to define extent of left atrial wall injury after the ablation of atrial fibrillation

Christopher J. McGann MD ³, Eugene G. Kholmovski PhD ³, Robert S. Oakes ^{1,2}, Joshua J.E. Blauer BS ^{1,2}, Marcos Daccarett MD¹, Nathan Segerson MD ¹, Kelly J. Airey MD ¹, Nazem Akoum MD ¹, Eric Fish ^{1,2}, Troy J. Badger ¹, Edward V.R. DiBella PhD ³, Dennis Parker PhD ³, Rob S. MacLeod PhD ^{1,2}, and Nassir F. Marrouche MD ¹

¹ Division of Cardiology, Internal Medicine. University of Utah School of Medicine.

² Bioengineering Department, University of Utah.

³ Radiology Department. University of Utah School of Medicine.

Corresponding Author:

Nassir F. Marrouche MD

Director, Atrial Fibrillation Program

Director, Electrophysiology Laboratory

Division of Cardiology

University of Utah Health Sciences Center

30 North 1900 East

Room 4A100

Salt Lake City, Utah 84132-2400

nassir.marrouche@hsc.utah.edu

Phone: +1-801-581-2572

Fax: +1-581-7735

Abbreviations

AF: Atrial fibrillation

LA: Left atrium

LV: Left ventricle

PVAI: Pulmonary vein antrum isolation

DE-CMRI: Delayed enhancement cardiac magnetic resonance imaging

RFA: Radiofrequency ablation

EA: Electro-anatomical

AAD: Anti-arrhythmic drugs

Abstract

Background. We describe a non-invasive method to detect and quantify left atrial (LA) wall injury after pulmonary vein antrum isolation (PVAI) in patients with atrial fibrillation (AF). Using a 3D delayed enhancement MRI sequence and novel processing methods, LA wall scarring is visualized at high resolution after radiofrequency ablation.

Methods and Results. LA wall imaging with a 3D delayed-enhanced cardiac MRI (DE-CMRI) sequence was performed pre and 3 months post ablation in 46 patients undergoing PVAI for AF. Our 3D, respiratory navigated, MRI sequence using parallel imaging resulted in 1.25 x 1.25 x 2.5 mm (reconstructed to 0.6 x 0.6 x 1.25 mm) spatial resolution with imaging times ranging 8-12 minutes. RF ablation resulted in clear hyper-enhancement of the LA wall in 100% of patients post PVAI and may represent tissue scarring. New methods to reconstruct the LA in 3D allowed quantification of LA scarring using automated methods. Arrhythmia recurrence at three months correlated with the degree of wall enhancement with > 13% injury predicting freedom from AF (OR=18.5 [CI 95% = 1.27 to 268], p =0.032).

Conclusions. We define non-invasive MRI methods that allows for the detection and quantification of left atrial wall scarring after RF ablation in patients with AF. Moreover, there seem to be a correlation between the extent of LA wall injury and short term procedural outcome.

Introduction

Atrial fibrillation (AF) is a growing clinical problem with enormous impact on both short-term quality of life and long-term survival (1,2). Radiofrequency ablation (RFA) to achieve Pulmonary Vein Antrum Isolation (PVAI) is a promising approach to cure AF. Controlled lesion delivery and scar formation within the LA are indicators of procedural success but the assessment of these factors is limited to invasive methods (3). As a result, a non-invasive evaluation of LA wall injury to assess permanent tissue injury may be an important step to improve procedural success.

Delayed enhancement cardiovascular magnetic resonance imaging (DE-CMRI) is an established non-invasive clinical method for characterizing tissue in a variety of cardiac disease processes including after myocardial infarction and injury due to myocarditis (4-11). Contrast enhancement in injured tissue using MRI occurs due to altered washout kinetics of gadolinium relative to the normal surrounding tissue. MRI has been successfully used to detect tissue injury due to RF lesion formation though data are limited. Animal studies have shown acute RF lesions in the right ventricle in dogs as a result of heat related changes in T1 and T2 parameters in the necrotic myocardium (12). RF lesion formation on the epicardium of dogs has also been characterized in several phases up to 12 hours post injury using gadolinium-enhanced MRI and RV enhancement correlated with histopathology showing coagulation necrosis with loss of cellular and vascular architecture (13). In humans, Peters et. al. reported on their initial experience using 3D DE-CMRI to detect LA scar 1-3 months after AF ablation and a case of left ventricular (LV) injury from previous RF ablation in a patient treated for idiopathic LV tachycardia has also been reported (14,15).

Though these data suggest MRI is well suited to provide important non-invasive evaluation of RFA lesions, human studies are lacking and its clinical role is still undefined. This study sought to detect and evaluate LA wall injury in patients with AF after PVAI using novel MRI methods and image

processing. Results shown here may help better define procedure outcome, guide follow up treatment, and develop strategies to avoid complications.

Methods

Patients

Fifty-three patients referred to the University of Utah for PVAI between December 2006 to July 2007 were enrolled in this study. The protocol was approved by the Institutional Review Board at the University of Utah and was HIPAA compliant. After informed consent was obtained, patients underwent pre-PVAI MRI scanning to define the PV's, location of the esophagus, LA anatomy, and for tissue characterization of the LA wall. MRI was repeated 3 months after ablation in all patients.

Following the procedure, patients continued anti-coagulation therapy with warfarin to maintain an international normalized ratio of 2.0 to 3.0 for a minimum of three months. Patients were assessed after three months to determine the success of the ablation procedure. Success was defined as a lack of late AF recurrence while off of antiarrhythmic medications. Event monitors were placed for a minimum of two months following their PVAI. Patients were instructed to activate the monitors any time they felt symptomatic. To confirm the absence of asymptomatic AF, all patients received a 48-hour Holter ECG recording at the 3-month follow-up. Recurrences were determined from patient reporting, event monitoring, Holter monitoring and ECG data. Recurrent AF was defined as a symptomatic or asymptomatic detected episode lasting > 15 seconds.

Pulmonary Vein Isolation Procedure

PVAI under intracardiac echocardiogram (ICE) guidance was performed. A 10 F, 64 element, phased array ultrasound catheter (AcuNav, Siemens; Mt. View) was used to visualize the inter-atrial septum and to guide the trans-septal puncture. A circular mapping catheter (Lasso, Biosense Webster; Diamond Bar, Colorado) and an ablation catheter were inserted into the LA. ICE was used to define

the PV ostia and their antra and to help position the circular mapping catheter and ablation catheter at the desired sites. Temperature and power were set to 50° and 50 W (pump flow rate at 30 cc/min), respectively. RF delivery was interrupted in the case of impedance rise or if a sudden increase in micro bubble density was observed during ablation. All study patients underwent PVAI, defined as electrical disconnection of the PV-antrum from the LA. Procedure methods have been published previously (16).

Delayed Enhancement MRI Acquisition Sequence

All participants underwent MRI studies on a 1.5 Tesla Avanto clinical scanner (Siemens Medical Solutions, Erlangen, Germany) using a TIM phased-array receiver coil 24 to 72 hours prior to PVAI. The protocol included sequences to define the anatomy of the LA and pulmonary veins. The anatomy was evaluated using the contrast enhanced 3D FLASH sequence and the cine true-FISP sequence. Typical acquisition parameters for 3D FLASH scan were: breath-hold in expiration, a transverse (axial) imaging volume with voxel size=1.25x1.25x2.5 mm, repetition time (TR) = 3.1 ms, echo time (TE) = 1.0 ms, and parallel imaging using the GRAPPA technique with reduction factor R=2 and 32 reference lines, scan time=14 sec. The 3D FLASH scan was acquired twice: pre-contrast and during a first pass of contrast agent (Multihance (Bracco Diagnostic Inc., Princeton, NJ), intravenous injection of a dose of 0.1 mmol per kilogram of body weight, 2 ml/sec injection rate, followed by a 15 ml saline flush). Timing of the first pass scan was defined using a MRI fluoroscopic scan.

Complete coverage of the LA was achieved with 16-22 transverse 2D slices acquired during retrospective electrocardiogram (ECG) gated, cine pulse sequence. All the images were acquired during breath-hold in expiration (1 or 2 slices per breath hold depending on the subject heart rate and tolerance to breath-holding) and were used to evaluate the LA morphology during the cardiac cycle. Typical scan parameters were: 6 mm slice thickness, no gap between slices, pixel size = 2.0 x 2.0 mm, TR/TE = 2.56/1.03 ms, GRAPPA with R=2 and 44 reference lines, 15 views per segment.

Delayed enhancement MRI (DE-CMRI) was used to identify fibrous tissue in the LA. DE-CMRI was acquired 15 minutes after the contrast agent injection using a 3D inversion recovery prepared, respiration navigated, ECG-gated, gradient echo pulse sequence. Typical acquisition parameters were: free-breathing using navigator gating, a transverse imaging volume with voxel size = 1.25 x 1.25 x 2.5 mm (reconstructed to 0.625 x 0.625 x 1.25 mm), TR/TE = 6.3/2.3 ms, inversion time (TI) = 230-270 ms, GRAPPA with R=2 and 32 reference lines. ECG gating was used to acquire a small subset of phase encoding views using during the diastolic phase of the LA cardiac cycle. The time interval between the R-peak of the ECG and the start of data acquisition was defined using the cine images of the LA. Fat saturation was used to suppress fat signal. The TE of the scan (2.3 ms) was chosen such that fat and water are out of phase and the signal intensity of partial volume fat-tissue voxels was reduced which allowed for improved delineation of the LA wall boundary. The TI value for the DE-CMRI scan was identified using a scout scan. Typical scan time for the DE-CMRI study was 5-10 minutes depending on subject respiration and heart rate. If the first acquisition did not have an optimal TI or had substantial motion artifacts, the scan was repeated.

Image Processing and Analysis

All MR images were evaluated and interpreted by two independent operators experienced in CMR imaging. Processing of the MRI DICOM formatted data sets were performed using OsiriX for visualization while quantification of images was performed using Matlab. LA data from 3D DE-CMRI acquisitions were evaluated slice-by-slice and utilizing volume rendering tools. These images were segmented and rendered which allowed for unique visualization of LA wall radiofrequency injury patterns using the entire data set and facilitated correlation with 3D CARTO images. Visualization was performed using smooth table opacity.

In patients who underwent post-procedural MRI scans, the relative extent of injury within the volume was measured using a threshold based lesion detection algorithm. In all images, the epicardial and endocardial borders were manually contoured using custom image display and

analysis software written in Matlab. Care was made in two-dimensional tracings of the endocardial and epicardial walls to confine the region of interest to only the LA wall and to avoid the blood pool, particularly on the right side, where a navigator induced artifact was present in some patient scans. Normal and injured tissue were defined based on a bimodal distribution of pixel intensities within the LA wall. The first mode of lower pixel intensities was chosen as normal tissue. Injured tissue was defined at 3 standard deviations above the normal tissue mean pixel intensity. Regions defined as lesion were visualized independently to ensure appropriateness of lesion detection. LA lesion area for each slice was summed for the entire scan and reported as a ratio of lesion volume to total LA wall volume. For selected patients with characteristic patterns of lesion formation observed in the Osirix 3D visualizations, image masks of injured regions were reconstructed into 3D volumes for comparison with the Osirix visualizations. The investigators were blinded during the analysis of all imaging and electrophysiology data.

Follow-up

All patients were monitored overnight on a telemetry unit after the procedure. Warfarin (INR 2-3) was restarted in all patients the day of PVAI, and was continued for a minimum of 3 months in paroxysmal, and for 6 months in persistent and permanent AF patients. Patients were followed in the outpatient clinic 3 months post-ablation, at which point they underwent an MRI scan to assess for PV stenosis, degree of chronic left atrial scarring, and Holter monitor recording for 24-48 hours.

Statistical Methods

Normal continuous variables are presented as mean \pm standard deviation. Continuous data were analyzed by student t-test to test for significant differences. Chi-square tests were used to test for differences in categorical measurements. Differences were considered significant at $p < 0.05$.

Statistical analysis was performed using the SPSS 15.0 Statistical Package (SPSS Inc.; Chicago, IL).

Results

Patients

Fifty-three patients who underwent PVAI for treatment of AF during the study period and completed the MRI scanning protocol were included in the analysis. Seven of the 53 patients were excluded due to inadequate MR images. The patients removed included six with poor image quality on the pre or post ablation scans and one who received an insufficient dose of IV contrast. Poor image quality resulted from patient motion and significant cardiac arrhythmia. In one case, navigator signal interference precluded accurate analysis. Results from the remaining forty-six patients were included in the data.

Table 1 shows the patient demographics for responders and non-responders to PVAI treatment. Statistically significant differences were seen among the study populations for age, left ventricular ejection fraction, LA area and LA volume and are consistent with prior published data (17-31).

Delayed Enhancement CMRI Visualization and Quantification

At baseline prior to ablation, no patients presented with hyperenhancement of the atrium prior to the procedure. It should be noted, however, that noticeable pre-ablation enhancement was seen in 4 patient scans (8.7%, however, the enhancement showed mild intensity and did not meet the previously published definitions of “hyperenhancement” as established in the ventricle, from which we developed the parameters for our quantification algorithm (32,33). In contrast, all (46 of 46, 100%) of the post-ablation images showed contrast enhancement most commonly in the posterior LA wall, interatrial septum, and surrounding the pulmonary veins (Figure 1). Two experienced, independent operators evaluated the presence or absence of contrast enhancement on DE-CMRI with agreement in all cases. Enhancement within the right pulmonary veins occurred in some patients. This was due

to the navigator radiofrequency pulse located over the right hemi-diaphragm and did not reflect tissue injury. This navigator-induced interference was differentiated from enhancement by its location and intensity. A recent change made to the pulse sequence has resulted in a complete removal of the navigator interference (data not shown).

Figure 1 shows MRI slices for four separate patients at baseline and three months post PVAI. As noted, the injury to the LA wall is largely located in the posterior wall, PV ostia and interatrial septum. However, degree of injury varied greatly between patients. The anterior LA wall was consistently spared and free of MRI evidence of injury in all patients, which is consistent with current strategies for catheter ablation of AF. Figure 1 also shows an example of 3D visualization of the LA wall in patient 1 pre and post ablation in four different orientations: posterior, right, left, and superior views.

Figure 2 shows LA injury detection using the semi-automated computer algorithm. When injury as identified by the computer algorithm is overlaid with 3D visualization (MIP), there is a strong correlation between the observed injury patterns and the region identified as scar by the algorithm. Figure 3 shows the overlay for one patient in three dimensions. LA injury identified by the computer algorithm (blue) matches regions of hyperenhancement (white) in the MRI visualization. Similar correlation between MRI visualization and algorithm detection were seen for all patients. This segmentation algorithm in conjunction with the DE-CMRI data allowed LA wall injury to be quantified as a percentage of the total LA wall volume.

Quantification of LA Wall Injury and Patient Outcome

At three months, 35 of 46 patients (76.1%) remained free of AF recurrence. All who suffered AF recurrences were placed back on anti-arrhythmic drugs. While a higher percentage of individuals who did not respond to therapy and suffered recurrence had persistent/permanent AF (8/11, 72.7%)

versus those who responded to therapy (16/35, 45.7%), this difference failed to reach statistical significance ($p = 0.118$).

A large difference was seen between the percentage of LA wall injury (as determined by MRI and semi-automated quantification) between responders and non-responders to PVAI. In patients who responded to ablation, the average LA wall injury was $19.3\% \pm 6.7\%$ while in those who did not respond the average LA wall injury was $12.4 \pm 5.7\%$ ($p = 0.004$). The strong association between average LA wall injury and recurrence persisted when stratifying patients by the first and second quartiles. Using the first quartile (LA wall injury $> 13\%$), patients with large scars were 18.5 times less likely to suffer recurrence of AF (OR=18.5 [CI 95% = 1.27 to 268], $p = 0.032$). After controlling for age, gender, ablation time and type of AF, large scar areas strongly predicted the absence of recurrences (adjusted OR = 83.7 [CI 95% = 2.013 to 3481.1], $p = 0.022$). Using the second quartile (median) as the cut off for large scar areas, the protective association between large scar areas and recurrences was smaller but still persisted ($p = 0.045$).

Discussion

Main Findings

In this study, we demonstrate LA injury after PVAI visualized by 3D DE-CMRI at high resolution using our novel imaging approach and processing methods. Left atrial wall injury resulting from RF ablation 3 months after PVAI was seen in every patient with tissue injury pattern reflecting location of RF energy delivery sites. In addition, injury on MRI appears to reflect tissue scarring and the degree of scarring correlates with procedural outcomes.

DE-CMRI Detects Tissue Injury from Radiofrequency Ablation

DE-CMRI is used routinely to accurately detect and size infarcted myocardium in patients with ischemic cardiomyopathy. It is arguably the gold standard viability study and accurately predicts

hibernating myocardium and response to revascularization (34,35). Performing DE-CMRI to detect LA wall injury is challenging as the LA is a thin wall structure compared to the LV and thus requires better spatial resolution while maintaining adequate CNR and SNR. The MRI pulse sequence we employ is a 3D high-resolution sequence similar to one reported on by Peters et. al. and achieves spatial resolution much greater than that typical for 2D delayed enhancement used in LV viability studies. In addition, we were able to take advantage of parallel imaging to significantly reduce the scan time and, as a result, reduce motion artifact.

Processing enhancements here greatly facilitated a more comprehensive evaluation of LA wall injury from images acquired from MRI images. Using a Dicom image editor, we developed methods to view the entire LA wall injury volume rendered in 3D from the slice data set which facilitated comparisons with other important 3D image data including CARTO derived voltage maps, sites of RF energy deposition, and the LA angiogram. Visualization of LA wall injury in 3D also improved assessment of lesion confluence and atrial debulking resulting from PVAI.

Injury patterns on DE-CMRI and Tissue Scarring in the LA

Effective injury to the LA wall and permanent tissue injury are important for procedural success.(36) Though invasive EA mapping is an important tool to help establish tissue ablation during the procedure, lesion recovery and incomplete sampling limit accurate and comprehensive assessment of permanent tissue injury. Non-invasive detection of LA wall injury using DE-CMRI is a recent advancement that reliably detected injury at three months in all of our patients (46/46 patients, no interobserver variability). In addition, the entire LA wall is visualized on 3D MRI and serial evaluation is safe and non-invasive.

There are a number of potential applications of our visualization technique and analysis. One such technique would analyze potential reasons for AF recurrence, such as that when loss of electrical isolation following pulmonary vein antrum isolation has occurred (37). Visualization of the

pulmonary veins and left atrium using three dimensional image processing allows for the scar pattern to be assessed and subsequent isolation procedures to be planned. Figure 5 shows visualizations of DE-MRI scans of two patients acquired three months following a failed PVAI (Figure 5, 1a-b and 2a-b).

These patients elected to undergo a second ablation procedure and had a second DE-MRI scan acquired following that procedure. Three dimensional segmentation of the LA was performed according to the described methods. Incomplete scar formation can be seen near the antrum of the pulmonary veins following the failed PVAI procedure. This gap in RF lesions at the pulmonary vein antrum (purple) correlated with incomplete electrical isolation of the left superior vein (as determined by EP study at the time of the second procedure). Following the repeat procedure, the MRI shows complete scar formation around the ostia of the left superior vein (Figure 5, 1c-d, 2c-d) in both patients. Three months following the second procedure, both patients were free of AF (as determined by 8 day holter recordings and patient self-report). In such an application, three dimensional processing provides an advantage over traditional 2D visualization as it allows for the spatial relationships and complex geometry of the LA to be better appreciated. This will likely lead to improved procedure planning and a lower recurrence rate of AF.

Left Atrial Wall Injury on MRI Predicted Procedural Outcome

Though all patients in this study had detectable injury on 3D DE-CMRI three months after ablation, the extent of injury varied significantly. When we applied our automated algorithm to quantify LA wall injury, degree of injury was significantly different between responders and non-responders (Table 2). After controlling for age, gender, AF phenotype, LA size, and LA volume, patients with scar ratios >13% are 18.5 times more likely to have a favorable outcome and freedom from AF at three months (OR=18.5 [CI95% 1.27 – 268], p=0.032). These data suggest that degree of LA wall scarring predicts procedural success. Our findings validate preliminary reports which appear to demonstrate that procedural outcome appears to correlate with overall enhancement (38).

The overall degree of scar may have important implications to the lesion type and subsequent interruption of PV to LA conduction. Interruption of PV to LA conduction has been an important component of procedural success. Verma et al. reported recurrent AF post PVAI in patients with more PV to LA conduction and shorter LA to PV delays. In comparison, the majority of patients maintaining sinus rhythm off AAD's showed no recurrent PV to LA conduction and significantly longer LA to PV delay (37). These results are supported by an earlier study by Ouyang et al. showing recovery of PV conduction in patients with recurrent atrial tachyarrhythmias after PVAI. Closing the conduction gaps on repeat procedure later successfully eliminated the arrhythmias (39). These data suggest that overall lesion permanence and complete PV isolation may be important procedural goals. The findings we present here appear also complimentary to this previous work and may indicate that degree of scarring on DE-CMRI may represent a non-invasive manner to estimate the atrial lesion type and the subsequent electrical isolation (37,39-41).

Study Limitations

Though the outcomes data in this study was statistically significant, the sample size was relatively small. In addition, 3D MR imaging in this study was performed on a 1.5 Tesla scanner. Significant improvements in LA wall imaging with greater spatial resolution, SNR and CNR is expected at higher magnetic field (3 Tesla). While we find found that the degree of atrial enhancement (and presumably scar) and freedom from recurrence were linked, we were not able to show whether this was due to complete and successful isolation at three months or simply due to the destruction of electrically viable tissue to such an extent that the atrium could no longer sustain atrial fibrillation. The standard ablation procedure at our facility incorporates both of these techniques and, as a result, we were unable to differentiate the relative contributions. Prospective studies designed to pursue this question should be pursued.

Conclusion

Non-invasive imaging of the LA wall with MRI is a recent advancement and powerful tool to evaluate injury related to radiofrequency energy delivery during AF ablation. Results reported in our study suggest that degree of left atrial wall injury predicts procedural outcome at three months.

Figures and Tables

Table 1. Patient Demographics - Summary by Response to Procedure

	Responders (n = 35)	Non-Responders (n = 11)	P-Value *
Type of Atrial Fibrillation			
Paroxysmal	19 (54.3%)	3 (27.3%)	0.118
Persistent	16 (45.7%)	8 (72.7%)	
Gender			
Female	12 (34.3%)	5 (45.5%)	0.503
Male	23 (65.7%)	6 (54.5%)	
Hypertension	18 (2.9%)	3 (27.3%)	0.161
Diabetes	5 (14.3%)	-	0.184
Coronary Artery Disease	4 (11.4%)	2 (18.2%)	0.562
History of Smoking	5 (17.1%)	4 (36.4%)	0.107
Valve Surgery	1 (2.8%)	-	0.571
Myocardial Infarct	2 (5.7%)	1 (9.1%)	0.692
Mitral Stenosis	4 (11.4%)	-	0.241
Age (Years)	63.1 ± 11.9	71.4 ± 11.4	0.048
Left Ventricular Ejection Fraction (%)	57.1 ± 4.9	49.5 ± 9.6	0.002
Left Atrial Area – Pre PVAI (cm ²)	20.1 ± 8.5	24.9 ± 6.4	0.147
Left Atrial Volume – Pre PVAI (cm ³)	84.8 ± 24.5	128.3 ± 29.8	< 0.001
Antiarrhythmic Medications			
None	19 (54.3%)	7 (63.6%)	0.567
One Medication	12 (34.3%)	2 (18.2%)	
Multiple Medications	4 (11.4%)	2 (18.2%)	

Table 2. Patients at 3 Month Follow-Up

	Responders (n = 35)	Non-Responders (n =11)	P-Value *
Percent Left Atrial Wall Injury	19.3 ± 6.7	12.4 ± 5.7	0.004
Degree of Scar Formation			
Minimal Scar Formation (Greater than 13% of Volume Enhancement)	3 (8.6%)	8 (72.7%)	< 0.001
Moderate Scar Formation (Less than 13% of LA Volume)	32 (91.4%)	3 (27.3%)	
Left Atrial Area (cm ²) – 3 Month Follow-up	18.0 ± 5.0	24.4 ± 4.6	< 0.001
Left Atrial Volume (cm ³) – 3 Month Follow-Up	74.1 ± 26.4	110.3 ± 16.8	< 0.001

Figure 1. Left atrial injury pre- and 3 months post-PVAI on 3D DE-CMRI. Left panels show LA wall slices at baseline (A) and 3 months post (B) PVAI on 3D navigated DE-CMRI in 4 different patients. Right panels show 3D rendering of LA in patient number 1 pre- and post-PVAI in multiple views (Posterior, Right, Left, and Superior) reconstructed from MRI slice data. Post-PVAI hyper-enhancement of LA wall is clearly seen (yellow arrows) in regions subjected to RF ablation and suggests scarring.

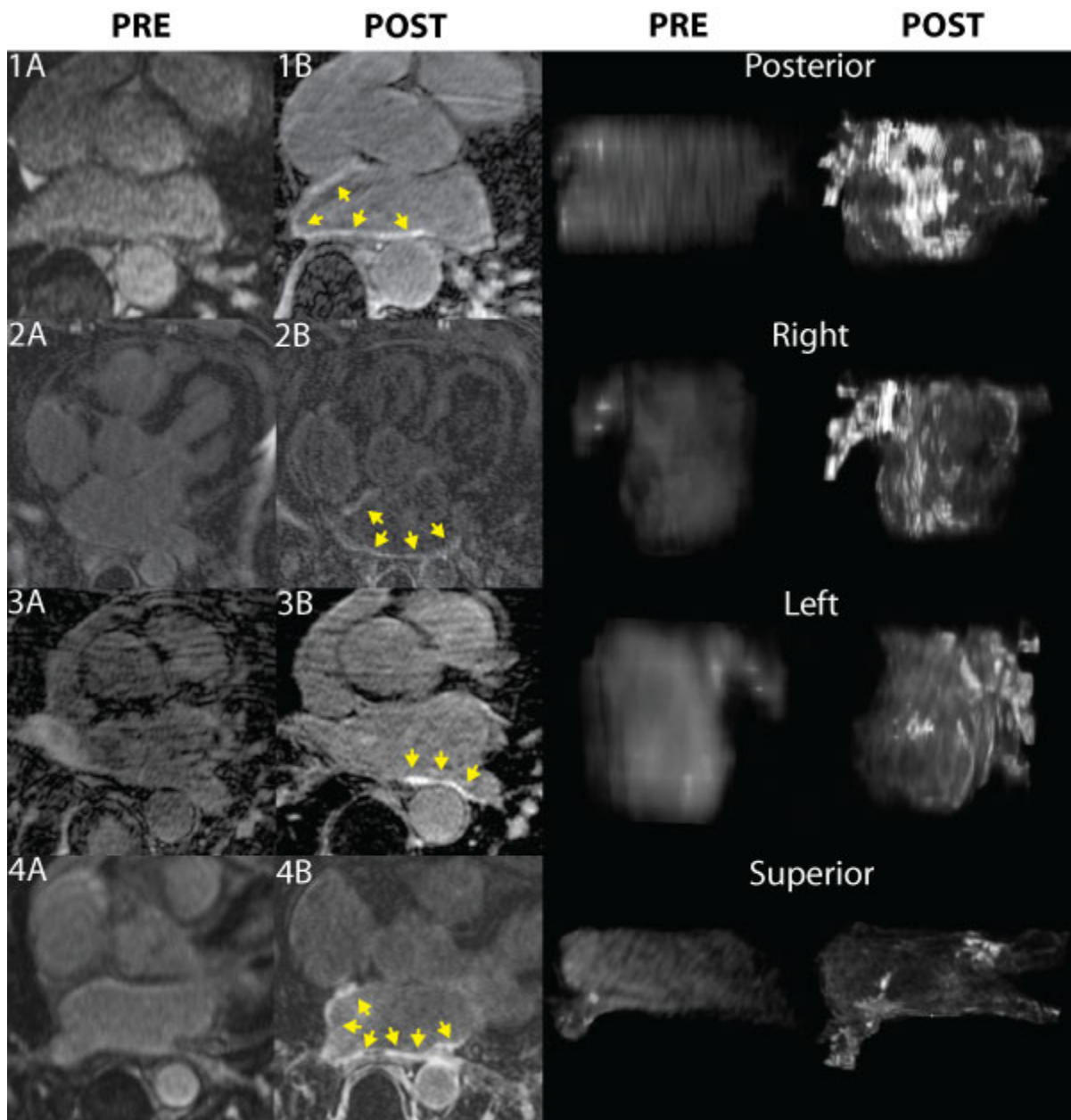


Figure 2. Automated quantification of chronic LA injury 3 months post PVAI. LA injury was determined using a threshold based on the defined normal regions of the LA wall. **Panels 1-16** show extent of injury at 5 standard deviations in a subset of slices from the 3D DE-CMRI from patient 1 (see figure 1). Reconstruction in 3D of the full set of data is shown in the right panels (**3D PA** and **RL** views). Using these methods, LA injury volume can be determined and calculated as a percentage of total LA wall volume.

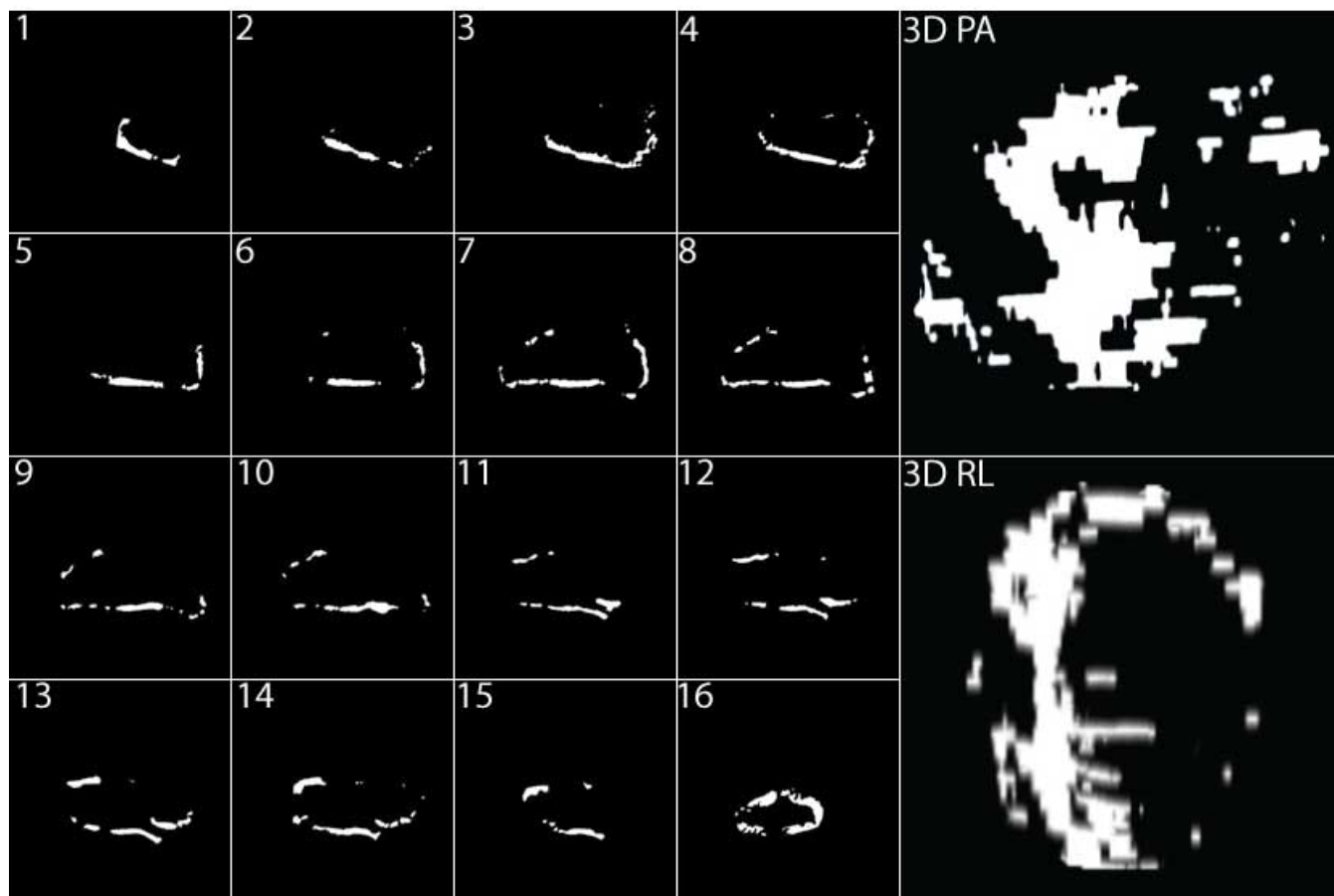


Figure 3. Overlay images of LA wall injury. **Panels 1a-d** are four example LA slices from the 3D DE-CMRI from patient 1 (see figure 1) that show close correlation of LA injury as determined by automated methods using a 3 SD cut-off value (**blue transparency**) overlaying MRI. Right panels show 3D overlay of full data set (**3D PA** and **RL**). LA injury mask (blue) determined by automated methods should match and overlay hyper-enhanced areas (**white**) of true injury on DE-CMRI. Though the left pulmonary veins are white on MRI, this enhancement is due to navigator interference, not injured tissue, as we position the navigator over the right hemi-diaphragm. The PV's are shown here only to help with anatomical orientation and are excluded from raw data used to produce injury mask by automated methods.

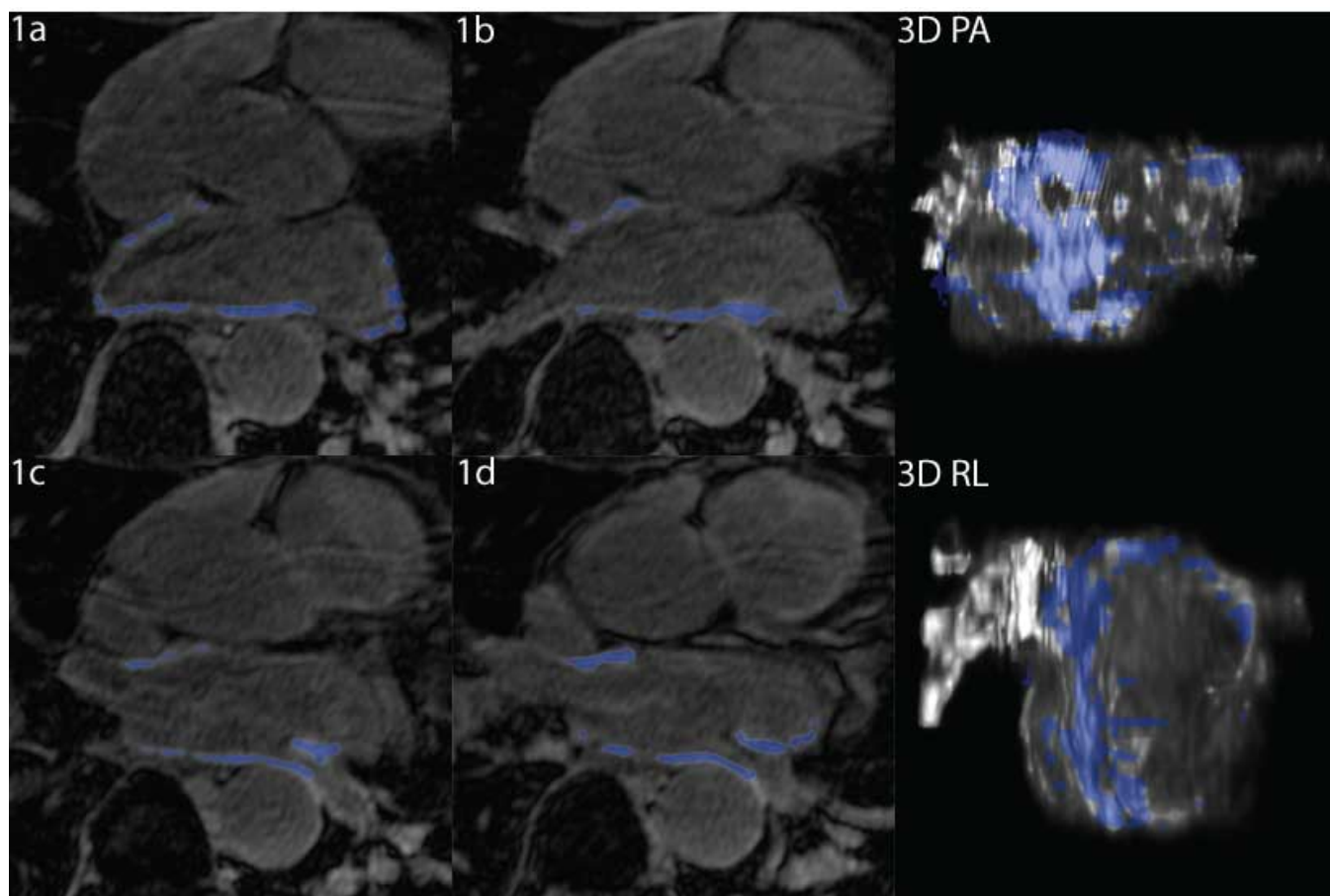


Figure 4. Association between atrial fibrillation recurrences and clinical success according to left atrial wall injury after catheter-based pulmonary vein antrum isolation. Patients with minimal scar formation at three months post procedure (> 13% of LA myocardial volume enhancement on DE-MRI) had a low procedural success and high recurrence of atrial fibrillation while patients with moderate scar formation at three months had a very high procedural success and low recurrence of atrial fibrillation.

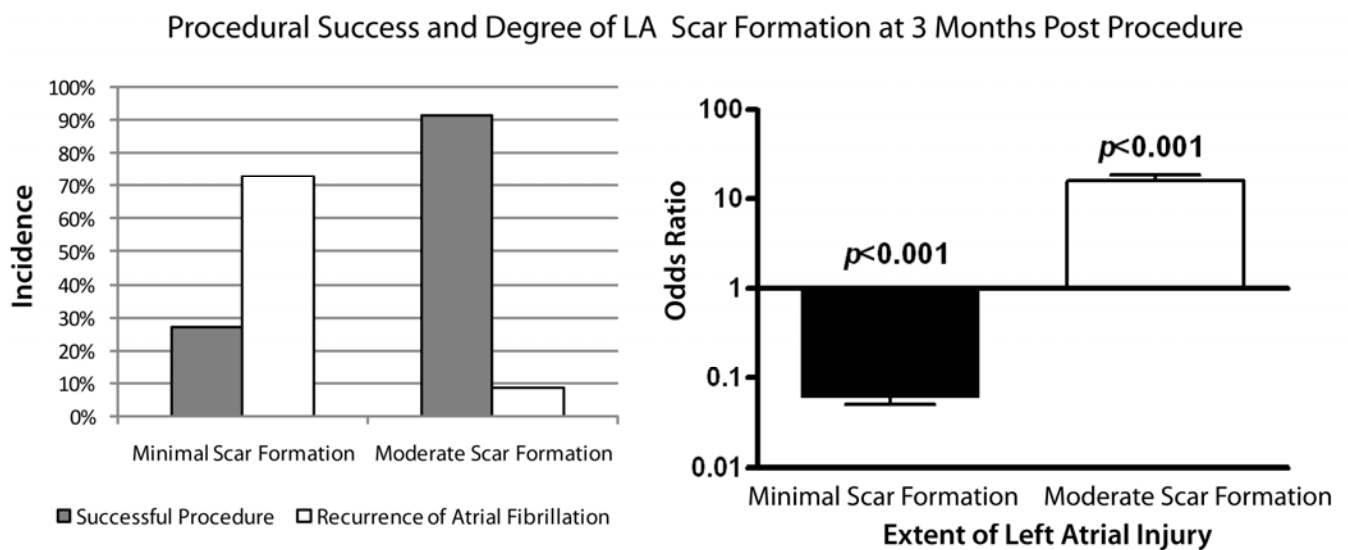
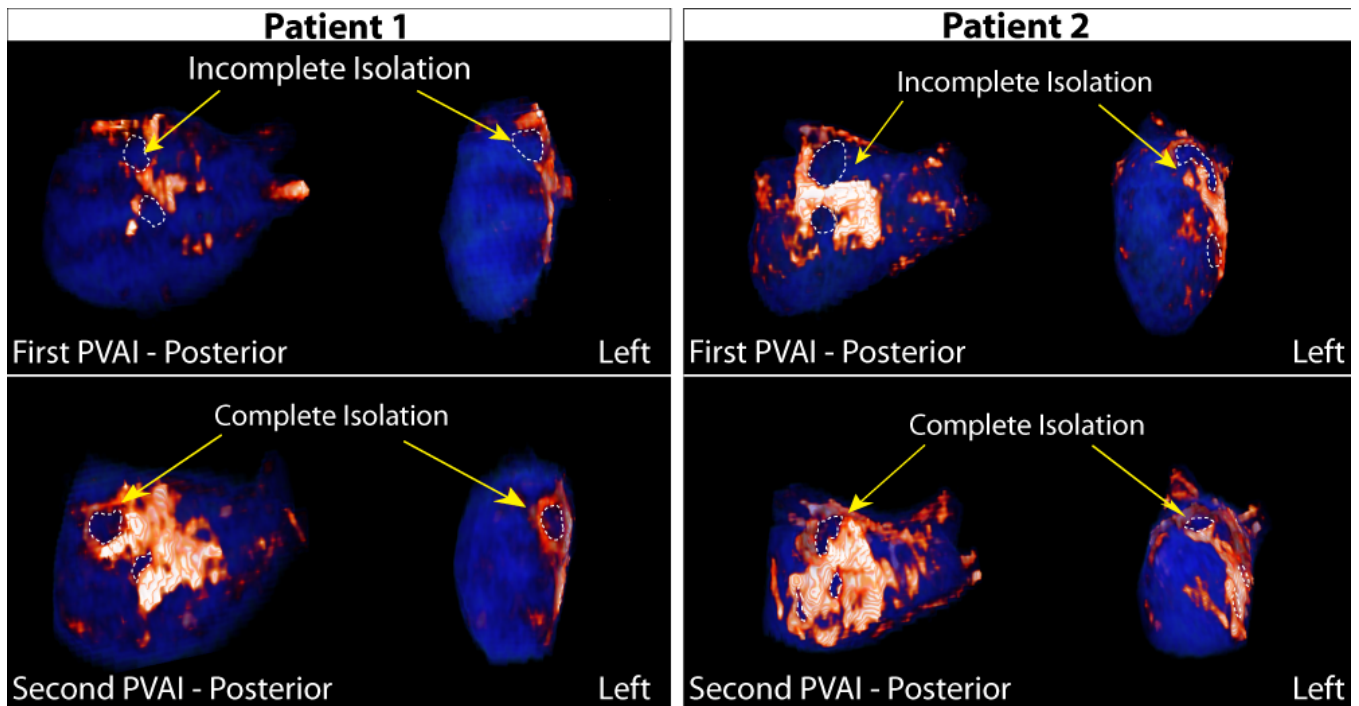


Figure 5. 3 month delayed enhancement MRI scans acquired 3 months following a first (failed) procedure (1a-b, 2a-b) and a second (successful) procedure (1c-d, 2c-d). Posterior (a) and left lateral views (b) are shown. Incomplete scar formation located near the antrum of the pulmonary veins following failed isolation was noted in both patients (1a-b, 2a-b). The gap in RF lesions at the pulmonary vein antrum (purple) correlated with incomplete electrical isolation of the left superior pulmonary vein. Delayed enhancement MRI at three months following the repeat PVAI shows complete scar formation (white/orange) isolating the pulmonary veins. Both patients were free of AF at follow-up.



References

1. Benjamin EJ, Wolf PA, D'Agostino RB, Silbershatz H, Kannel WB, Levy D. Impact of atrial fibrillation on the risk of death: the Framingham Heart Study. *Circulation* 1998;98:946-52.
2. Dries DL, Exner DV, Gersh BJ, Domanski MJ, et al. Atrial fibrillation is associated with an increased risk for mortality and heart failure progression *Journal of the American College of Cardiology* 1998.
3. Oh S, Kilicaslan F, Zhang Y, et al. Avoiding microbubbles formation during radiofrequency left atrial ablation versus continuous microbubbles formation and standard radiofrequency ablation protocols: comparison of energy profiles and chronic lesion characteristics. *J Cardiovasc Electrophysiol* 2006;17:72-7.
4. Kim RJ, Fieno DS, Parrish TB, et al. Relationship of MRI delayed contrast enhancement to irreversible injury, infarct age, and contractile function. *Circulation* 1999;100:1992-2002.
5. Klein C, Nekolla SG, Bengel FM, et al. Assessment of myocardial viability with contrast-enhanced magnetic resonance imaging: comparison with positron emission tomography. *Circulation* 2002;105:162-7.
6. Kim RJ, Wu E, Rafael A, et al. The Use of Contrast-Enhanced Magnetic Resonance Imaging to identify Reversible Myocardial Dysfunction. *N Engl J Med* 2000;343:1445-1453.
7. De Cobelli F, Pieroni M, Esposito A, et al. Delayed gadolinium-enhanced cardiac magnetic resonance in patients with chronic myocarditis presenting with heart failure or recurrent arrhythmias. *J Am Coll Cardiol* 2006;47:1649-54.
8. Rochitte CE, Tassi EM, Shiozaki AA. The emerging role of MRI in the diagnosis and management of cardiomyopathies. *Curr Cardiol Rep* 2006;8:44-52.
9. Laissy JP, Hyafil F, Feldman LJ, et al. Differentiating acute myocardial infarction from myocarditis: diagnostic value of early- and delayed-perfusion cardiac MR imaging. *Radiology* 2005;237:75-82.
10. Oshinski JN, Han HC, Ku DN, Pettigrew RI. Quantitative prediction of improvement in cardiac function after revascularization with MR imaging and modeling: initial results. *Radiology* 2001;221:515-22.
11. Mahrholdt H, Goedecke C, Wagner A, et al. Cardiovascular magnetic resonance assessment of human myocarditis: a comparison to histology and molecular pathology. *Circulation* 2004;109:1250-8.
12. Lardo AC, McVeigh ER, Jumrussirikul P, et al. Visualization and temporal/spatial characterization of cardiac radiofrequency ablation lesions using magnetic resonance imaging. *Circulation* 2000;102:698-705.
13. Dickfeld T, Kato R, Zviman M, et al. Characterization of radiofrequency ablation lesions with gadolinium-enhanced cardiovascular magnetic resonance imaging. *J Am Coll Cardiol* 2006;47:370-8.
14. Peters DC, Wylie JV, Hauser TH, et al. Detection of pulmonary vein and left atrial scar after catheter ablation with three-dimensional navigator-gated delayed enhancement MR imaging: initial experience. *Radiology* 2007;243:690-5.
15. Sievers B, Brandts B, Moon JC, Pennell DJ, Trappe HJ. Cardiovascular magnetic resonance of iatrogenic ventricular scarring due to catheter ablation for left ventricular tachycardia. *Int J Cardiol* 2003;91:249-50.

16. Kanj MH, Wazni O, Fahmy T, et al. Pulmonary vein antral isolation using an open irrigation ablation catheter for the treatment of atrial fibrillation: a randomized pilot study. *J Am Coll Cardiol* 2007;49:1634-41.
17. Pritchett AM, Jacobsen SJ, Mahoney DW, et al. Left atrial volume as an index of left atrial size: a population-based study. *Journal of the American College of Cardiology* 2003.
18. Natale A, Newby KH, Pisano E, et al. Prospective randomized comparison of antiarrhythmic therapy versus first-line radiofrequency ablation in patients with atrial flutter. *J Am Coll Cardiol* 2000;35:1898-904.
19. Wazni OM, Marrouche NF, Martin DO, et al. Radiofrequency ablation vs antiarrhythmic drugs as first-line treatment of symptomatic atrial fibrillation: a randomized trial. *JAMA* 2005;293:2634-40.
20. Karch MR, Zrenner B, Deisenhofer I, et al. Freedom from atrial tachyarrhythmias after catheter ablation of atrial fibrillation: a randomized comparison between 2 current ablation strategies. *Circulation* 2005;111:2875-80.
21. Oral H, Pappone C, Chugh A, et al. Circumferential pulmonary-vein ablation for chronic atrial fibrillation. *N Engl J Med* 2006;354:934-41.
22. Gaita F, Riccardi R, Caponi D, et al. Linear cryoablation of the left atrium versus pulmonary vein cryoisolation in patients with permanent atrial fibrillation and valvular heart disease: correlation of electroanatomic mapping and long-term clinical results. *Circulation* 2005;111:136-42.
23. Haissaguerre M, Hocini M, Sanders P, et al. Catheter ablation of long-lasting persistent atrial fibrillation: clinical outcome and mechanisms of subsequent arrhythmias. *J Cardiovasc Electrophysiol* 2005;16:1138-47.
24. Sanders P, Morton JB, Davidson NC, et al. Electrical remodeling of the atria in congestive heart failure: electrophysiological and electroanatomic mapping in humans. *Circulation* 2003;108:1461-8.
25. Nademanee K, McKenzie J, Kosar E, et al. A new approach for catheter ablation of atrial fibrillation: mapping of the electrophysiologic substrate. *J Am Coll Cardiol* 2004;43:2044-53.
26. Haissaguerre M, Sanders P, Hocini M, et al. Catheter ablation of long-lasting persistent atrial fibrillation: critical structures for termination. *J Cardiovasc Electrophysiol* 2005;16:1125-37.
27. Willems S, Klemm H, Rostock T, et al. Substrate modification combined with pulmonary vein isolation improves outcome of catheter ablation in patients with persistent atrial fibrillation: a prospective randomized comparison. *Eur Heart J* 2006;27:2871-8.
28. Calo L, Lamberti F, Loricchio ML, et al. Left atrial ablation versus biatrial ablation for persistent and permanent atrial fibrillation: a prospective and randomized study. *J Am Coll Cardiol* 2006;47:2504-12.
29. Kistler PM, Rajappan K, Jahngir M, et al. The impact of CT image integration into an electroanatomic mapping system on clinical outcomes of catheter ablation of atrial fibrillation. *J Cardiovasc Electrophysiol* 2006;17:1093-101.
30. Sauer WH, McKernan ML, Lin D, Gerstenfeld EP, Callans DJ, Marchlinski FE. Clinical predictors and outcomes associated with acute return of pulmonary vein conduction during pulmonary vein isolation for treatment of atrial fibrillation. *Heart Rhythm* 2006;3:1024-8.
31. Chugh A, Oral H, Lemola K, et al. Prevalence, mechanisms, and clinical significance of macroreentrant atrial tachycardia during and following left atrial ablation for atrial fibrillation. *Heart Rhythm* 2005;2:464-71.

32. Hsu LY, Natanzon A, Kellman P, Hirsch GA, Aletras AH, Arai AE. Quantitative myocardial infarction on delayed enhancement MRI. Part I: Animal validation of an automated feature analysis and combined thresholding infarct sizing algorithm. *J Magn Reson Imaging* 2006;23:298-308.
33. Hsu LY, Ingkanisorn WP, Kellman P, Aletras AH, Arai AE. Quantitative myocardial infarction on delayed enhancement MRI. Part II: Clinical application of an automated feature analysis and combined thresholding infarct sizing algorithm. *J Magn Reson Imaging* 2006;23:309-14.
34. Kim RJ, Wu E, Rafael A, et al. The use of contrast-enhanced magnetic resonance imaging to identify reversible myocardial dysfunction. *N Engl J Med* 2000;343:1445-53.
35. Knuesel PR, Nanz D, Wyss C, et al. Characterization of dysfunctional myocardium by positron emission tomography and magnetic resonance: relation to functional outcome after revascularization. *Circulation* 2003;108:1095-100.
36. Kistler PM, Ho SY, Rajappan K, et al. Electrophysiologic and anatomic characterization of sites resistant to electrical isolation during circumferential pulmonary vein ablation for atrial fibrillation: a prospective study. *J Cardiovasc Electrophysiol* 2007;18:1282-8.
37. Verma A, Kilicaslan F, Pisano E, et al. Response of atrial fibrillation to pulmonary vein antrum isolation is directly related to resumption and delay of pulmonary vein conduction. *Circulation* 2005;112:627-35.
38. Peters DC, Wylie JV, Hauser TH, et al. Abstract 3371: Recurrence of Atrial fibrillation Following RF Ablation Correlates with the Extent of Post-procedural Left Atrial Scarring on Delayed-Enhancement CMR. *Circulation* 2007;116:II_760-d-761.
39. Ouyang F, Antz M, Ernst S, et al. Recovered pulmonary vein conduction as a dominant factor for recurrent atrial tachyarrhythmias after complete circular isolation of the pulmonary veins: lessons from double Lasso technique. *Circulation* 2005;111:127-35.
40. Gerstenfeld EP, Dixit S, Callans D, et al. Utility of exit block for identifying electrical isolation of the pulmonary veins. *J Cardiovasc Electrophysiol* 2002;13:971-9.
41. Ouyang F, Ernst S, Chun J, et al. Electrophysiological findings during ablation of persistent atrial fibrillation with electroanatomic mapping and double Lasso catheter technique. *Circulation* 2005;112:3038-48.